PROGRESS IN PHOTOVOLTAICS: RESEARCH AND APPLICATIONS
Prog. Photovolt: Res. Appl. 2008; **16**:577–584
Published online 9 July 2008 in Wiley InterScience (www.interscience.wiley.com) DOI: 10.1002/pip.840

Research

Study of Base Series Resistance Losses in Single and Double Emitter Silicon Solar Cells Through Simulations and Experiments

K. Kotsovos*,† and K. Misiakos
Institute of Microelectronics, NCSR Demokritos, P. O Box 60228, 153 10 Aghia Paraskevi, Attiki, Greece

This work focuses on base series resistance influence on the performance of single and double emitter rear point contact silicon solar cells. This study is performed through measurements on experimental devices with different rear contact sizes and spacings, which were designed and fabricated using standard silicon integrated circuit technology, while the results were compared with simulation data based on a 3D model developed at our institute. Simulation and experimental results show that the series resistance of the double junction structure is significantly lower compared to the single junction equivalent. In addition, it was demonstrated that the operation of both junctions under slightly different voltages improves device efficiency. Copyright © 2008 John Wiley & Sons, Ltd.

KEY WORDS: silicon; point contact; double junction; series resistance; 3D simulation

Received 31 October 2007; Revised 20 March 2008

INTRODUCTION

During the last two decades, the evolution of silicon solar cell technology as well as the design of novel structures has led to significant improvements in device conversion efficiency. One of the most advanced devices was the rear point contact solar cell, developed at Stanford University[1] in order to be used for concentrator systems. In addition, this structure demonstrated the highest one-sun efficiency (22·3%) among other silicon solar cell structures in 1988.[2] Its main advantages compared to conventional solar cells are low front and back surface recombination and minimal series resistance-shadowing losses, since all metal contacts are located on the back surface, while the whole front area and most of the rear are passivated with high-quality thermal oxide. Amonix Inc. has developed solar cells based on this design that are capable of generating power with 27·6% efficiency under 100× concentration.[3] However, this design is too complex and expensive for use at low concentrations and SunPower Corporation has developed a simplified process for that purpose, providing solar cells fabricated on high-quality FZ substrates with efficiencies greater than 20% under normal sunlight.[4] The choice of a high-quality material is necessary for

* Correspondence to: K. Kotsovos, Institute of Microelectronics, NCSR Demokritos, P. O Box 60228, 153 10 Aghia Paraskevi, Attiki, Greece.
†E-mail: kotsovos@imel.demokritos.gr

this type of solar cells, since the photogenerated carriers need to reach the back surface in order to be collected.

Another advanced structure is the passivated emitter rear locally diffused (PERL) solar cell,[5] which was developed in the University of New South Wales (UNSW) and has demonstrated the highest efficiency (24·7%) under AM1·5 illumination.[6] This device has many improvements compared to conventional solar cells (passivated emitter in the front surface, advanced light trapping, contact passivation, while the back area is covered with oxide and rear metal contacts are performed through small openings in it to minimize recombination losses). However an important limiting factor of the efficiency of PERL cells is the increased series resistance due to current crowding at the back contacts, which results to fill factor losses. Therefore, the optimization of the back contact spacing and coverage fraction was necessary to suppress these effects, so extensive simulations in two and three dimensions have been performed in the literature[7–11] for that purpose.

A less common variation of the PERL and the point-contact solar cell is the double junction rear point contact structure, a device with an additional emitter on the back surface. This device is based on the double-sided n^+-p-n^+ device proposed by Luque *et al.* for concentrator applications,[12] while Warabisako *et al.*[13] fabricated a similar device on polycrystalline silicon substrates. The additional emitter on the back surface (which is electrically connected with the front one) improves the photocurrent of the cell; thus high-quality substrates are not required for efficient carrier collection. A double junction rear point contact structure—also called bifacial triode cell since it has three terminals—was designed by Ohtsuka *et al.*,[14] where this device reached the highest efficiency under bifacial illumination. The triode cell was also proposed as the optimal structure when illuminated from both surfaces compared to other bifacial solar cells, since it provides more output power.[15] In addition, the triode structure showed significantly less light degradation compared to other bifacial structures due to enhanced carrier collection from the back emitter.[16]

Since rear point contact solar cells show a higher efficiency potential compared to conventional back contacting schemes, due to reduced surface recombination, the double junction solar cell and the PERL device have been investigated by means of simulations, using our developed 3D model.[17] Single and double emitter structures have also been compared through 1D and 2D simulations.[18] The present work is a detailed study of base series resistance losses in rear point contact structures with single and double-sided emitters. Simulation results are compared with measurements on experimental single front and double junction rear point contact devices developed at the institute of microelectronics, NCSR Demokritos. In addition, the operation of the double emitter solar cell under slightly different front and back junction voltages (as a triode device) is investigated.

DEVICE FABRICATION

The devices are fabricated on double-polished 4″ p-type Czochralski (Cz) wafers with a resistivity of 1 Ω.cm and thickness of 380 μm. Photolithography was used to define the emitter areas, front and back (interdigitated) finger grid and rear point contacts; seven photomasking steps were performed, using a double-sided mask aligner. The junctions were formed through phosphorus ion implantation, while the local back surface field at the point contacts was created by boron implantation. A double layer antireflective coating consisting of a 57 nm thick Si_3N_4 film and 110 nm SiO_2 on top has been formed on the front surface of the cells. The films were formed by LPCVD deposition. The back surface of the single junction cell is covered with a thick (500 nm) thermal oxide and square holes according to the geometry shown in Figure 1a are opened in it through photolithography to form the point contacts. Several different combinations of back point contact sizes and distances were examined.

The double junction solar cell's back emitter covers the entire rear area excluding the point contacts and a small oxide region surrounding them, which serves as an isolation layer between emitter and back contacts (Figure 1b). Solar cell active area is 0·49 cm^2 (0·7 × 0·7 cm), while device dimensions are 0·9 × 0·9 cm, as shown in Figure 2a, due to the metal frame of 1 mm width, which surrounds the cell. Therefore, emitter areas do not extend under the metal frame. In addition, front emitter electrodes were designed thin (12 μm) and closely spaced (94 μm), while there is also a horizontal busbar in the middle of the structure, to further reduce finger grid resistance. Figure 2b shows an optical microscope photo detail of the interdigitated back metal design. Since back junction photocurrent is a small fraction compared to the front one, back emitter electrode width is much

DOI: 10.1002/pip

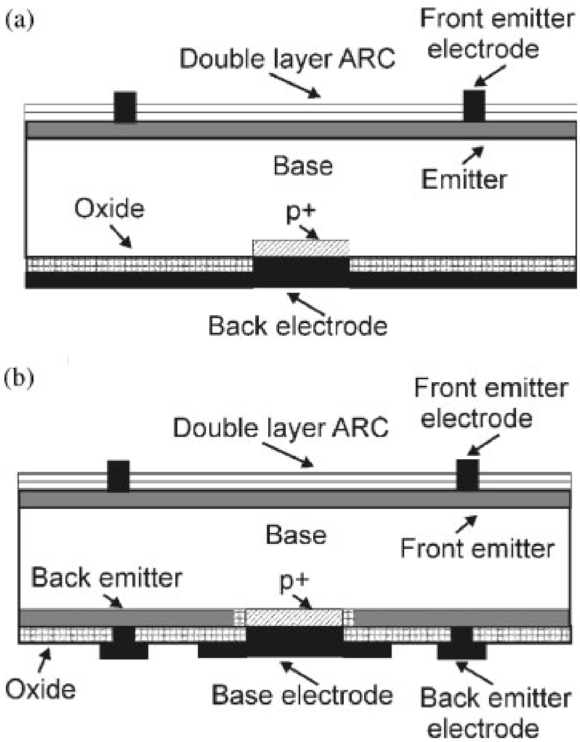

Figure 1. Structure of the experimental rear point contact solar cells: (a) single junction and (b) double junction device. The point contacts are squares with sidelength d and are repeated with distance l

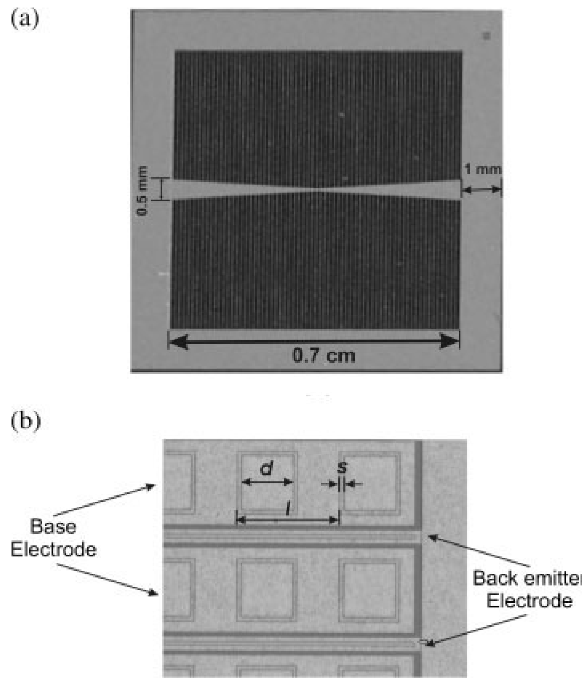

Figure 2. Front (a) and back surface (b) photograph of an experimental double junction solar cell. Point contacts are squares with sidelength d and distance l, while the frame of width s is the oxide isolated area between the back emitter and the base contacts

smaller. In order to ensure a high back metal coverage, the spacing between back emitter and base contacts is dense (2–4 μm, depending on the point contact distance). The rear point contacts and the frame of width s that surrounds them (isolation area between back emitter and base contact) can also be observed in this figure. The design of front and back electrodes was focused in minimizing series resistance losses, despite the increased shading (13·2% front active area shadowing). In this way, back emitter and metal series resistance is negligible, while the corresponding contribution of the front metal and emitter is only 7 mΩ. Therefore, the solar cell region where series resistance losses mainly occur is the base, so their dependence on rear point contact size and spacing could be investigated in detail.

RESULTS

The cell series resistance (R_s) is evaluated through measurements under illumination and in the dark. For the dark current measurement a larger voltage (V_{dark}) than V_{oc} is required in order to obtain a current with the same value as the short circuit current (I_{sc}) due to series resistance voltage drop. Therefore, R_s can be obtained by the difference between these voltages

$$R_s = \frac{V_{dark} - V_{oc}}{I_{sc}} \tag{1}$$

In order to eliminate parasitic resistances from the measuring system, we used the "4 point probe technique" to ensure accurate voltage measurements.

Due to the complex device geometry of rear point contact structures, a 3D model was developed by solving the minority and majority carrier transport equations in the base of the investigated structure. The simulation method is based on transforming the horizontal (x, y) dimensions in the basic partial differential equations by two-dimensional fast Fourier transform (FFT) while the vertical dimension (z) is kept continuous. In this way there is a considerable reduction in calculation time and memory requirements since only 2D discretization is needed, thus the whole solar cell I–V curve may be easily obtained in a typical PC. The basic required assumptions are planar geometry and low injection, while emitter and front grid series resistance losses are considered negligible. This method and the corresponding simulation algorithm are described in reference[11] Through this algorithm the voltage drop due to majority carrier transport is calculated and base series resistance can be obtained. The calculation of R_s through the simulation program is obtained from the evaluated I–V curve near the maximum power point using the following relation:[11]

$$R_s = \frac{V_{oc} - V - \frac{KT}{e}\ln\frac{I_{sc}}{I_{sc} - I}}{I} \tag{2}$$

where K is the Boltzmann constant, e the electronic charge, and T is the temperature of the cell. This formula allows a direct calculation of the series resistance from the illuminated solar cell I–V curve, without requiring the calculation of the dark current characteristic. Both expressions result in the same R_s values as shown in Table I. This table was calculated by simulating the dark and illuminated I–V curves of single emitter devices with various back contact sizes and spacing 400 μm. The parameters used in the calculations were those of the experimental devices. The small differences in series resistance values when calculated with the two different expressions are expected since all I–V curves were extracted with steps of 1 mV accuracy, in order to avoid exhaustive computations. Due to the relative low minority carrier diffusion length of the Cz substrates used (200 μm), both open circuit voltage and photocurrent are almost independent of back contact size.

The following graphs show a comparison of the simulated and measured series resistance of single and double junction solar cells as a function of back point contact size d to distance l ratio (d/l) when l is 400 and 200 μm. The right axis is the series resistance of the point contact structures normalized to the corresponding simulated conventional 1D n^+-p-p^+ one (base contact is performed on the whole back surface). The graphs show a rapid increase in series resistance when d/l ratio is less than 0·25 due to intense current crowding effects around the back contacts.[6] In addition, R_s of the double junction structure is significantly lower compared to the single junction equivalent, a result already observed earlier through our simulation model.[17] Good agreement between experimental and simulated results is found, which is clearly shown in Figure 3a, while Figure 3b shows that there is an increased scattering of experimental points mainly in the case of the double junction structure, since due to its very low series resistance, measured dark and light voltages differ very slightly (in the order of 1 mV or less), thus increasing measurement errors. In addition, the right axis values show that R_s of the double junction structure is lower than the conventional 1D solar cell when back contact coverage is medium or large, depending on their spacing l ($d/l = 0{\cdot}5$ if $l = 400$ μm or $d/l > 0{\cdot}2$ if $l = 200$ μm). In order to investigate the influence of back emitter on base carrier transport, we evaluated the series resistance of the back junction structure (a device where there is only one emitter located in the whole back surface, excluding the rear contacts) and compared its value through simulations on the single front and double junction solar cell, as a function of the rear point contact size (d/l ratio), as shown in Figure 4a. The schematic of the simulated back emitter device is illustrated in Figure 4b. The plots show that the back junction solar cell is the device with the lowest R_s, followed by the double junction equivalent. Therefore the location of an emitter in the back surface results in reduced series

Table I. Series resistance values of the single emitter structure calculated through expressions (1) (R_{s1}) and (2) (R_{s2}) applied to simulated dark and illuminated I–V curves under different back point contact sizes and constant spacing 400 μm

d (μm)	J_{sc}(mA/cm^2)	J_d (mA/cm^2)	R_{s1} (Ω.cm^2)	R_{s2} (Ω.cm^2)	V_{oc} (mV)	V_{dark} (mV)
40	35·628	35·365	0·198	0·197	604	611
50	35·626	35·783	0·164	0·157	604	610
80	35·619	35·798	0·111	0·099	604	608

J_{sc}, V_{oc} are the short circuit current and open circuit voltage respectively, while V_{dark} is the dark I–V voltage that corresponds to a current J_d (ideally) equal to J_{sc}. The simulated parameters correspond to the experimental structures: thickness 380 m, base doping $N_A = 1{\cdot}38 \times 10^{16}\,cm^{-3}$ (corresponding to a resistivity of 1 Ω.cm), emitter recombination current $J_0 = 10^{-12}$ A/cm^2 (estimated through dark I–V curves), base diffusion length $L_n = 200$ m.

DOI: 10.1002/pip

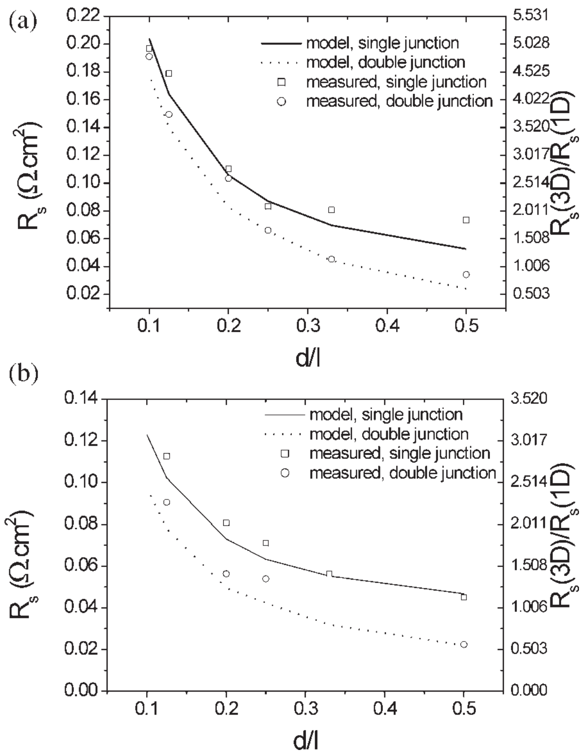

Figure 3. Simulated and measured series resistance of single and double junction rear point contact solar cells as a function of *d/l* ratio, for two different contact distances: 400 μm (a) and 200 μm (b). The right axis is the series resistance of the point contact structure normalized to the corresponding conventional one

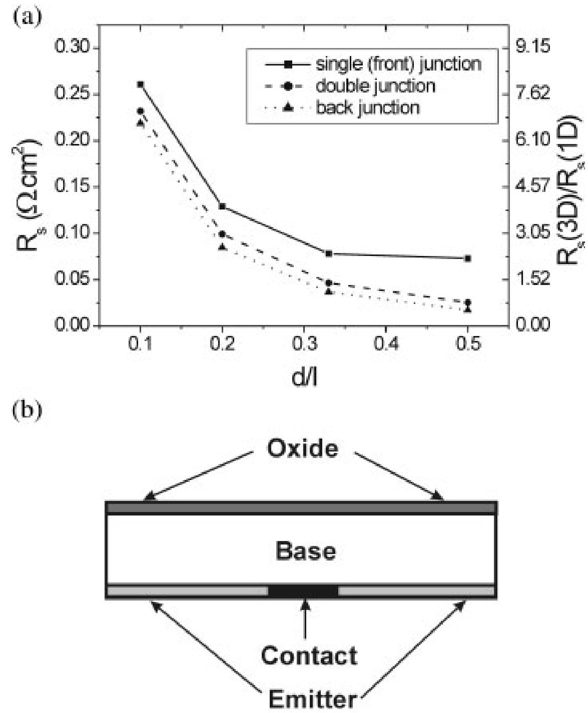

Figure 4. (a) Simulated series resistance comparison of the single, double and back junction (a structure where the emitter is located on the back surface only) solar cell devices as a function of the *d/l* ratio, where back point contact spacing is 400 μm, while cell thickness is 400 μm and base doping concentration is 10^{16} cm^{-3}. (b) Schematic of the simulated back junction solar cell

resistance losses. This is an important asset when concentrator applications are considered, where large device operating currents require minimal series resistance losses for efficient solar cell operation. In addition, the double emitter structure has the additional advantage of improved photocurrent collection compared to the other two devices. In contrast, the back junction solar cell requires high base diffusion lengths for efficient carrier collection, restricting its fabrication on expensive substrates. In other words, the double junction solar cell combines the advantages of both low series resistance and high photocurrent.

In order to estimate the importance of base resistance losses under higher illumination levels in single and double emitter rear point contact solar cells, a series of simulations were performed under low concentration (10 suns maximum). The selected structures are 400 μm thick, while minority carrier diffusion length is 800 μm, which corresponds to low bulk recombination. Base doping density is 10^{16} cm^{-3} and emitter recombination current is 10^{-13} A/cm^2, which corresponds to a well-passivated emitter. Back contact spacing and sidelength was set as 200 μm and 20 μm respectively. Simulations under high concentration were not performed since in that case our model assumption of low-level injection would not be valid. Figure 5a shows the efficiency of the two different structures as a function of light concentration. The graphs show that under normal illumination (1 sun) the single emitter structure performs better due to reduced recombination on the back surface. When concentration levels increase however, the double emitter structure demonstrates a significantly higher efficiency. Series resistance influence is demonstrated in Figure 5b where solar cell maximum voltage versus concentration is plotted. The graph shows that V_m is affected to a greater extent in the single emitter device due to increased base resistance losses. Another issue is the reduction of efficiency as well as maximum voltage when illumination levels are higher than

DOI: 10.1002/pip

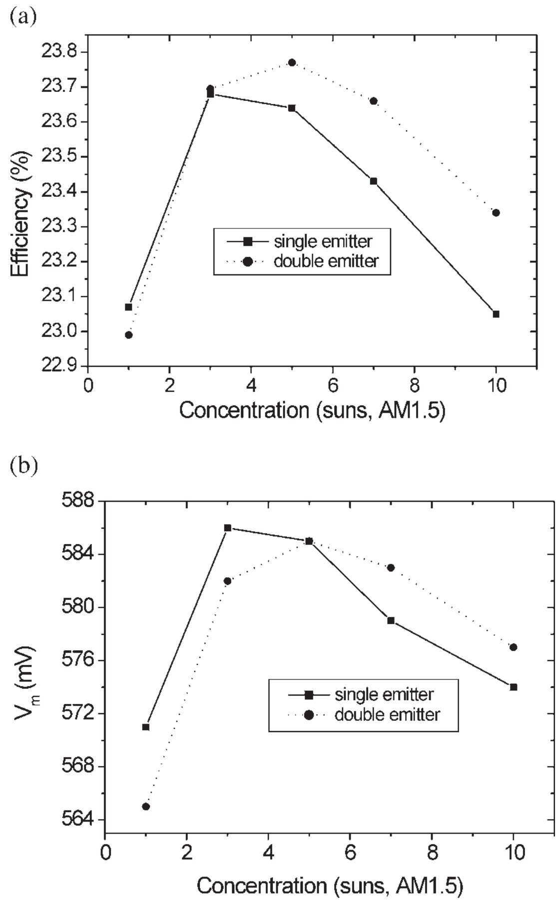

Figure 5. (a) Simulated efficiency comparison of the single and double emitter structures as a function of light concentration, where back point contact spacing is 200 μm, cell thickness is 400 μm, and base doping is $10^{16}\,cm^{-3}$. (b) Maximum power point voltage versus light concentration.

5 suns, indicating that base resistance seriously degrades solar cell performance. Therefore, solar cell back contact geometry as well as base thickness must be optimized for reduced series resistance, when concentrator applications are considered.

Since the double junction solar cell is a three-terminal device, we investigated its operation when front and back emitters were biased under different potential. The next figure is a plot of the double junction solar cell power output (normalized to the value obtained when both emitters are on the same potential) as a function of the measured voltage difference between the back and front emitter when the current on the back emitter is constant (0·2 mA), while on the front junction variable. Both emitter

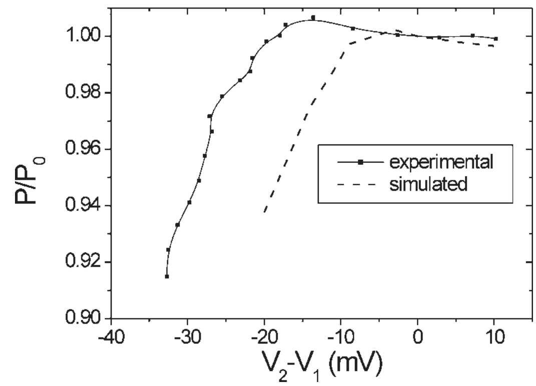

Figure 6. Normalized power output of the double junction solar cell as a function of front and back emitter potential difference (V_2-V_1), where V_2 and V_1 are the back and front junction voltage respectively, and P_0 is the device power when $V_2 = V_1$. The supplied current on the back emitter is 0·2 mA. Back contact spacing and size are: $l = 400$ μm and $d = 40$ μm, while solar cell thickness is 400 μm.

current bias points were selected near the measured maximum power point of the cell. The plot of Figure 6 shows that the maximum power of the cell is observed when the junctions are biased under different voltages. The measured maximum is reached when back emitter voltage is 13·57 mV less than the front one. A simulated curve obtained under similar conditions is also added in this graph. The observed differences between these curves may be attributed to spectral differences and slight intensity variations between experimental illumination source and the simulated AM1·5 spectrum. Although the efficiency improvement shown in Figure 6 is rather insignificant, if both junction potentials are changed under a wider range of voltages, a greater increase in device performance could be found. The curves of Figure 7 examine the effect of different emitter potentials on the performance of a simulated double junction solar under the same device parameters of the previous figure. In the first curve (solid line), front junction bias voltage (V_1) is kept constant at a value that corresponds to the simulated maximum power point of the cell (V_{mpp}) when both emitters are biased with the same potential ($V_1 = V_2$), while the second one (dashed) is calculated at a front emitter potential 30 mV less. The first plot shows that by decreasing the back junction voltage (V_2) up to 60 mV compared with the front one, the efficiency increases and beyond this value it starts to saturate. This improvement is more than 0·5% (absolute). The second curve, however, shows an

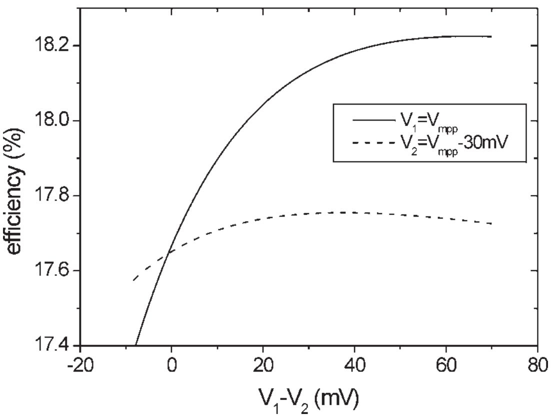

Figure 7. Simulated power output (normalized) of the double junction solar cell as a function of front and back emitter potential difference for the device parameters of Figure 6. The graphs are obtained under constant front emitter voltage ($V_1 = V_2$), while the back one is varied. Two different cases are considered: (1) $V_1 = V_{mpp}$, where V_{mpp} is the maximum power point when both emitters are connected under the same voltage and (2) $V_1 = V_{mpp}$-30 mV

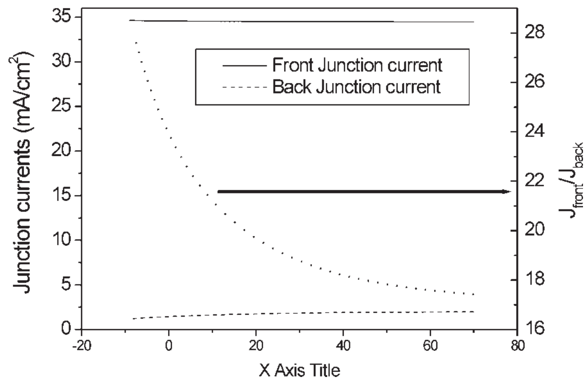

Figure 8. Junction currents as a function of voltage difference between front and back emitter (V_1-V_2) for the cell parameters of Figure 7 (first case). On the right axis the value of front to back current ratio is shown (dot curve)

obviously reduced improvement with a broad maximum at approximately 40 mV difference. These results indicate that the maximum efficiency gain is more sensitive to the front junction potential since the front emitter delivers most of the power. However, if device parameters change to an extent that back emitter collection efficiency increases (e.g. higher minority carrier diffusion length and/or lower base thickness), then back junction potential should influence maximum efficiency in a different way as observed in reference[17] where devices with high diffusion length (800 μm) are considered.

Further analysis may be performed by examining the current collected from both junctions for the case of Figure 7 (when $V_1 = V_{mpp}$). This is shown in Figure 8, where the left axis shows the current values while the right shows the front to back junction current ratio. The graphs show a significant increase in the back junction current followed by decrease in the front junction current when back emitter potential drops. This change is rapid for the initial 20 mV voltage difference. Therefore, the analysis of these two figures leads to the conclusion that a more balanced split of the photocurrent between the two junctions increases the efficiency. This result can be expected since ohmic power losses depend on the square of the current and the front junction delivers most of it, so a proper balance of junction currents by controlling both emitter potentials may lead to optimal solar cell performance.

CONCLUSIONS

In this work single and double junction rear point contact silicon solar cells were studied through series resistance measurements on experimental structures fabricated at the institute of microelectronics, NCSR Demokritos. Series resistance measurements were in good agreement with simulation results based on our 3D model. In addition, it was shown that due to the back emitter, the double junction structure exhibited reduced series resistance losses compared to the single front junction equivalent and conventional back contact solar cell, setting it as a more suitable choice for concentrator systems. Finally, simulation results and experimental measurements indicated that operation of both emitters under slightly different voltages leads to device efficiency increase.

REFERENCES

1. Swanson RM. Point-contact solar cells: modelling and experiment. *Solar Cells* 1986; **17**: 85–118.
2. King RR, Sinton RA, Swanson RM. Front and back surface fields for point contact solar cells. *20th IEEE Photovoltaic Specialists Conference*, Las Vegas, USA, 1988; 538–544.
3. Slade A, Garboushian V. An improved high-concentration silicon solar cell and its implication for the mass production of high concentration PV systems. *Proceedings of*

the 21st EPVSEC, Dresden, Germany, 2006; 769–772.
4. Mulligan W, Rose D, Cudzinovic MJ, De Ceuster DM, McIntosh, KR, Smith DD, Swanson RM. Manufacture of solar cells with 21% efficiency. *Proceedings of the 19th EPVSEC*, Paris, France, 2004; 387–390.
5. Wang A, Zhao J, Green MA. 24% efficient silicon solar cells. *Applied Physics Letters* 1990; **57**: 602–604.
6. Zhao J, Wang A, Green MA. 24.5% efficiency PERT cells on MCZ substrates and 24.7% efficiency PERL cells on FZ substrates. *Progress in Photovoltaics: Research and Applications* 1999; **7**: 471–474.
7. Zhao J, Wang A, Green MA. Series resistance caused by the localized rear contact in high efficiency silicon solar cells. *Solar Energy Materials and Solar Cells* 1994; **32**: 89–94.
8. Aberle AG, Heiser G, Green MA. Two-dimensional numerical optimization study of the rear contact geometry of high-efficiency silicon solar cells. *Journal of Applied Physics* 1994; **75**: 5391–5405.
9. Heiser G, Aberle AG. Numerical modeling of non-ideal current-voltage characteristics of high-efficiency silicon solar cells. *5th IEEE Workshop on Numerical Modelling of Processes and Devices for Integrated Circuits (NUPAD V)*, Hawaii, USA, 1994; 177–180.
10. Catchpole KR, Blakers AW. Modelling the PERC structure for industrial quality silicon. *Solar Energy Materials and Solar Cells* 2002; **73**: 189–202.
11. Kotsovos K, Misiakos K. Three-dimensional simulation of carrier transport effects in the base of rear point contact silicon solar cells. *Journal of Applied Physics.* 2001; **89**: 2491–2496.
12. Luque A, Cuevas A, Ruiz JM. Double-sided n^+-p-n^+ for bifacial concentration. *Solar Cells* 1980; **2**: 151–166.
13. Warabisako T, Matsukuma K, Kokunai S, Kida Y, Uematsu T, Yagi H. Bifacial multicrystalline silicon solar cells. *23rd IEEE Photovoltaic Specialists Conference*, Louisville, USA, 1993; 248–251.
14. Ohtsuka H, Sakamoto M, Tsutsui K, Yazawa Y. Bifacial silicon solar cells with 21.3% front efficiency and 19.8% rear efficiency. *Progress in Photovoltaics: Research and Applications* 2000; **8**: 385–390.
15. Ohtsuka H, Sakamoto M, Koyama M, Tsutsui K, Uematsu T, Yazawa Y. Characteristics of bifacial solar cells under bifacial illumination with various intensity levels. *Progress in Photovoltaics: Research and Applications* 2001; **9**: 1–13.
16. Ohtsuka H, Sakamoto M, Koyama M, Muramatsu S, Yazawa Y, Warabisako T, Abe T, Uematsu T, Saitoh T. Effect of light degradation on bifacial Si solar cells. *Solar Energy Materials and Solar Cells* 2001; **66**: 51–59.
17. Kotsovos K, Misiakos K. Base limited carrier transport and performance of double junction rear point contact silicon solar cells. *Solar Energy Materials and Solar Cells* 2003; **77**: 209–227.
18. Kerschaver E, Van Zechner C, Dicker J. Double sided minority carrier collection in silicon solar cells. *IEEE Transactions on Electron Devices* 2000; **47**: 711–717.